repeated separation and purification steps by preparative GLC, until a constant value of the specific activity of each component, measured by liquid scintillation counting (Tri-Carb 460 C, Packard Instrument Co.) was reached. The yield of each labeled product was deduced from the ratio of its activity to the total activity of the [^{3}H]phenylium ions formed within the system during the storage period, as calculated from the initial activity of [1,4-$^3H_2$]benzene and its known decay rate. The gas chromatographic analyses were carried out with the following columns: (a) Bentone 34-diisodecyl phthalate (1:1 on Chromosorb, W, 1 m) + Carbowax 20 M (15% on Chromosorb W, 3 m), T_c = 60-130 °C; (b) tricresyl phosphate (20% on Chromsorb W-AW-DMCS, 8 m), T_c = 100-120 °C.

Degradation of Tritiated Products. The tritium distribution within the tritiated halobenzenes recovered from the decay samples was determined by a procedure based on the replacement of a ^{3}H of the product by an inactive substituent, followed by the measurement of the corresponding decrease of the molar activity. Substitution reactions were chosen to minimize the danger of label losses or shifts due to unwanted isotopic exchange processes, as demonstrated by blank degradations carried out on suitably deuterated precursors. Chlorination of chlorobenzene carried out in the presence of powdered iron gave a mixture of isomeric dichlorobenzenes which was resolved by preparative GLC on a Bentone 34 column (2 m, 120 °C) and a DC 550 silicone oil column (4 m, 130 °C). The same reaction carried out on fluorobenzene provided *o*- and *p*-chlorofluorobenzene, which were resolved on a Bentone 34 column (2 m, 110 °C) and a tricresyl phosphate column (4 m, 110 °C), and the activity of the purified isomers was measured. The *p*-chlorofluorobenzene was then nitrated (HNO_3/H_2SO_4) and the 2-chloro-5-fluoronitrobenzene was separated with a Bentone 34 column (1 m, 120 °C). Bromobenzene was treated with $Cl_2/AlCl_3$ at 60 °C to give isomeric bromochlorobenzenes which were separated from the starting material with a DC 550 silicone column (2 m, 100 °C). The isomeric bromochlorobenzenes were resolved with a Bentone 34-diisodecyl phthalate 1:1 column (1 m, 110 °C).

Registry No. 1, 82235-88-9; **2**, 73728-29-7; CH_3F, 593-53-3; CH_3Cl, 74-87-3; CH_3Br, 74-83-9; CH_3OH, 67-56-1.

High Resolution Electron Energy Loss Vibrational Studies of CO Coordination to the (10$\bar{1}$0) Surface of ZnO

K. L. D'Amico,[1a] F. R. McFeely,*[1b] and Edward I. Solomon*[2]

Contribution from the Department of Chemistry, Massachusetts Institute of Technology, Cambridge, Massachusetts 02139, and Department of Chemistry, Stanford University, Stanford, California 94305. *Received May 2, 1983*

Abstract: High Resolution Electron Energy Loss Spectroscopy (HREELS) has been used to study the interaction of CO with the (10$\bar{1}$0) ZnO surface. The results presented represent the first successful effort to use HREELS to measure the vibrations of CO on any single crystal metal oxide surface and serve as a complement to our earlier photoelectron spectroscopic studies of the CO/ZnO system. Observation of the intraligand C-O stretching mode (273 meV, 2202 cm^{-1}) and its first overtone (539 meV, 4348 cm^{-1}) verify that the CO molecule adsorbed at low coverages under ultrahigh-vacuum (UHV) conditions on (10$\bar{1}$0) is indeed the same "high frequency" CO observed on ZnO powders. In addition, observation of the Zn-C metal-ligand stretch (31 meV, 250 cm^{-1}) enables application of a normal mode calculation which indicates that the majority of the increased CO stretching frequency is due to an increase in the CO force constant and not just due to mechanical coupling to the surface. These results are discussed in light of the mechanism of methanol synthesis on ZnO.

Introduction

The CO-ZnO system is of significant interest both with respect to its inorganic chemistry and its reactivity. First, zinc oxide is an effective catalyst in taking CO and H_2 to methanol.[3] Further, the CO-ZnO surface complex is rather unusual in that it requires carbon monoxide bonding to a coordinatively unsaturated surface containing metal ions in higher oxidation states surrounded by oxide ligands; this is in contrast to the more usual zero valent metal surfaces where structural analogies to organometallic complexes can be drawn. Associated with this unusual inorganic complex are some rather unusual spectral features which may reflect differences in electronic structure and reactivity. In particular, as opposed to metals where CO binding results in a decrease of the intraligand stretching frequency relative to its gas-phase value due to charge transfer from the metal d orbitals to the $2\pi^*$ orbital on the CO, on ZnO powders the CO stretching frequency increases from 2143 to ~2200 cm^{-1}.[4]

A variety of chemical and spectroscopic studies[5] on four single crystal ZnO Surfaces employing He(II) ultraviolet photoelectron spectroscopy (UPS) have generated the CO binding geometry on the ZnO (10$\bar{1}$0) surface shown in Figure 1. Here, CO is binding carbon end down approximately along the coordinatively unsaturated Zn direction but tilted somewhat toward the coordinatively unsaturated surface oxide ion. (The unsaturated Zn direction is 19° off normal while the CO has been determined to bind 30° off normal.) A correlation of the geometric structure of the CO-ZnO active site to the electronic structure requires further insight into the vibrational spectrum of this complex. This has been pursued at a single crystal level in ultra high vacuum (UHV) on the (10$\bar{1}$0) ZnO surface through High Resolution Electron Energy Loss Spectroscopy (HREELS).

In contrast to the wide range of current literature pertaining to HREELS studies of clean and adsorbate covered metal surfaces, there have been relatively few such studies on single crystal metal oxides. Ibach has extensively studied the clean ZnO surface by HREELS, measuring the Fuchs-Kliewer surface phonon spec-

(1) (a) Massachusetts Institute of Technology. Presently at Physics Department, Brookhaven National Laboratory, Upton, NY 11973. (b) Massachusetts Institute of Technology. Presently at Thomas J. Watson Research Center, IBM, Yorktown Heights, NY 10598.

(2) Stanford University.

(3) F. Boccuzzi, E. Garrone, A. Zechina, A. Bossi, and M. Camia, *J. Catal.*, **51**, 160 (1978).

(4) A. L. Waddams, "Chemicals from Petroleum", 3rd ed; Wiley, New York, 1973.

(5) (a) R. R. Gay, M. H. Nodine, E. I. Solomon, V. E. Henrich, and H. J. Zeiger, *J. Am. Chem. Soc.*, **102**, 6752 (1980); (b) M. J. Sayers, M. R. McClellan, R. R. Gay, E. I. Solomon, and F. R. McFeely, *Chem. Phys. Lett.*, **75**, 575 (1980); (c) M. R. McClellan, M. Trenary, N. D. Shinn, M. J. Sayers, K. L. D'Amico, E. I. Solomon, and F. R. McFeely, *J. Chem. Phys.*, **74**, 4726 (1981); (d) K. L. D'Amico, M. Trenary, N. D. Shinn, E. I. Solomon, and F. R. McFeely, *J. Am. Chem. Soc.*, **104**, 5102 (1982).

0002-7863/83/1505-6380$01.50/0

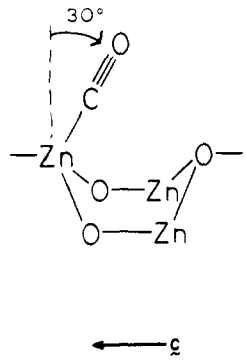

Figure 1. The binding geometry of CO on the (10$\bar{1}$0) ZnO surface determined by UPS and ARPES studies (ref 5).

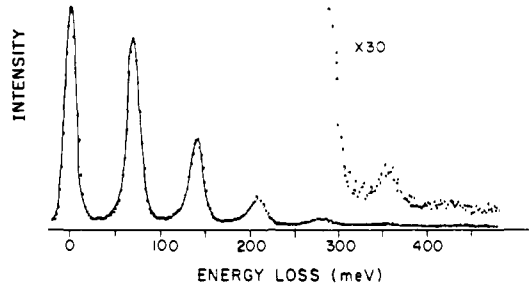

Figure 2. HREELS spectrum of the clean ZnO (10$\bar{1}$0) surface at T = 100 K. Resolution of the elastic peak is ~15 meV. Impact energy is ~4.5 eV.

trum.[6] Unfortunately, it is the predominance of this phonon structure which has frustrated attempts to use HREELS for direct observation of adsorbate vibrations on metal oxide surfaces.[7] Recent studies by Goldstein et al.[8] on the interaction of adsorbed atomic hydrogen with the vibrational modes of the clean (000$\bar{1}$) ZnO surface have provided evidence for the existence of two-dimensional plasma oscillations in the resultant accumulation layer; these coupled plasmon–phonon modes manifest themselves by a temperature-dependent broadening of the clean surface energy loss features (vida infra); however, no evidence of discrete chemisorbed hydrogen vibrations was reported. The results presented here represent the first successful effort to use HREELS to measure the vibrations of CO on any single crystal metal oxide surface and thus serve to complement our earlier photoemission studies of this important methanol catalyst.

Experimental Section

A standard stainless steel ion pumped UHV chamber, equipped with Physical Electronics 4-grid LEED/Auger optics, was employed. Base pressure was ~ 2×10^{-10} torr. The HREELS spectrometer was a cylindrical deflection instrument, as described by Sexton.[9] Beam current at the crystal was ~3×10^{-11} A.

The experiments reported here were performed on surfaces prepared by two different methods. The majority of the results were obtained on a crystal which was cleaved in air and heated to 700 K.[7,8] These results were checked against crystals which were cut and polished and subjected to argon bombardment and annealing cycles as in previous studies.[5,7a,10] In all cases the results were essentially identical.

All spectra were recorded at a surface temperature of 100 K, as the width of the surface phonon features is narrowest at lower temperatures. This is due to the presence of low-frequency modes, resulting from the adsorption of less than 1% of a monolayer of atomic hydrogen,[8] which are depopulated at lower temperatures thus causing the phonon features to sharpen considerably. ZnO surfaces are well-known for their ability to adsorb atomic hydrogen, which is produced by the action of any hot tungsten filament (electron gun, mass spectrometer, ion gauge, etc.) upon the molecular hydrogen background generally present in any ion-pumped stainless steel UHV chamber.[11]

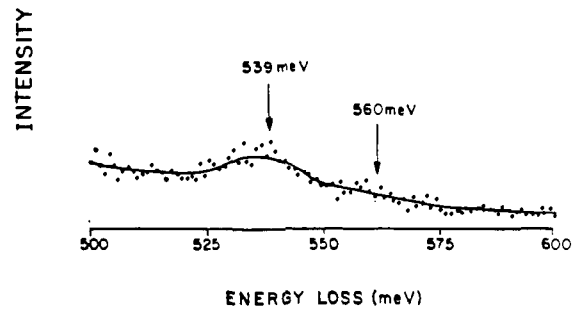

Figure 3. HREELS spectrum of the CO-covered surface at T = 100 K, 500–600 meV loss region. The loss feature at 539 meV (4348 cm^{-1}) is due to the 1st overtone of the CO intraligand stretch. The arrow indicates the position where the n = 8 phonon loss peak is expected to occur, illustrating that the peak at 539 meV is due to the adsorbed CO.

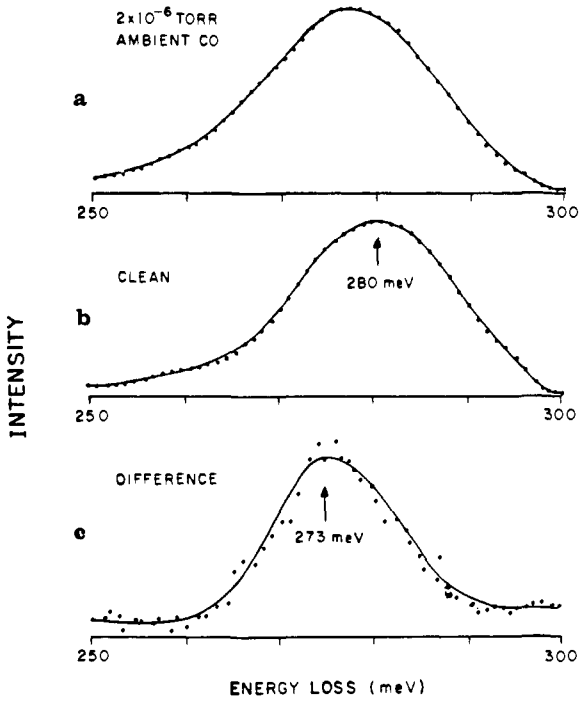

Figure 4. HREELS spectra in the 250–300 meV loss region at T = 100 K: (a) CO-covered surface; ambient pressure of 2×10^{-6} torr; (b) clean surface; (c) difference curves of the 273 meV (2202 cm^{-1}) CO intraligand stretch.

Results and Discussion

Figure 2 shows the HREELS spectrum of the clean surface at T = 100 K for a beam voltage of ~4.5 eV. For this and all other spectra reported here the angle of incidence was 60° and detection was in the specular direction. The features at ~70-meV intervals are due to multiple excitations of the Fuchs–Kliewer surface phonons. The relative intensities of these modes are known to be impact-energy dependent, becoming stronger at lower impact energy.[6] We have observed up to the 7th overtone of this mode for an impact energy of 1.5 eV.

No change in this phonon structure is observed when CO is adsorbed on the surface (ambient CO pressure = 2×10^{-6} torr);[12] however, three new loss features develop due to the presence of

(6) (a) H. Ibach, *Phys. Rev. Lett.*, **24**, 1416 (1970); (b) H. Ibach, *J. Vac. Sci. Technol.*, **9**, 713 (1972); (c) A. Many, J. I. Gersten, I. Wagner, A. Rosenthal, and Y. Goldstein, *Surf. Sci.*, **113**, 355 (1982).

(7) (a) J. L. Gland, Exxon Research Labs, private communication; (b) A. Orchard, Oxford University, private communication.

(8) (a) Y. Goldstein, A. Many, I. Wagner, and J. Gersten, *Surf. Sci.*, **98**, 599 (1980); (b) A. Many, I. Wagner, A. Rosenthal, J. I. Gersten, and Y. Goldstein, *Phys. Rev. Lett.*, **46**, 1648 (1981).

(9) B. A. Sexton, *J. Vac. Sci. Technol.*, **16**, 1033 (1979).

(10) J. D. Levine, A. Willis, W. R. Bottoms, and P. Mark, *Surf. Sci.*, **29**, 144 (1972).

(11) K. Haberrecker, E. Mollwo, H. Schreiber, H. Hoinkes, H. Nahr, P. Lindner, and H. Wilsch, *Nucl. Instrum. Methods*, **57**, 22 (1967).

(12) There is also no change in the phonon structure for GaAs when atomic hydrogen or atomic deuterium is adsorbed, even though discrete losses due to Ga–H(D) and As–H(D) are seen. See: H. Lüth and R. Matz, *Phys. Rev. Lett.*, **46**, 1652 (1981).

Table I. Comparison of Stretching Frequencies and Calculated Force Constants for Adsorbed and Gas-Phase CO

surface	structure[a]	ν_{CO}[b] meV	ν_{CO}[b] cm^{-1}	ν_{M-C}[b] meV	ν_{M-C}[b] cm^{-1}	calcd[i] k_{M-C}	calcd[i] k_{CO}
Pt(111)[d]	C(4X2)	261	2105	60	484	4.19	16.41
Cu(100)[e]	C(2X2)	260	2097	43	347	2.02	17.05
Ni(100)[f]	C(2X2)	256.5	2069	59.5	480	3.98	15.87
ZnO(10$\bar{1}$0)[g]	[c]	273 ± 2	2202	31 ± 1	250	1.01	19.21
gas phase		265.7	2143				18.56[j]

[a] Values for stretching frequencies are for CO bound on top for all four surfaces. [b] Frequencies in meV; 1 meV = 8.065 cm^{-1}. [c] Adsorbed CO shows no LEED evidence for the formation of an ordered overlayer (see ref 5a). [d] Reference 15. [e] Reference 16. [f] Reference 17. [g] This work. [h] Reference 18. [i] Force constants in mdyn/Å. [j] Reference 19.

adsorbed CO. Figure 3 shows the 500–600-meV region of the adsorbate-covered surface, in which a weak feature (intensity 5 × 10^{-4} times that of the elastic beam) is apparent at 539 meV (4348 cm^{-1}). For this value of impact energy (~4.5 eV) the clean surface loss spectrum is flat in this region. This feature is assigned as the first overtone of the CO stretching frequency; assuming zero anharmonicity, this would predict a CO fundamental frequency of 270 meV (2178 cm^{-1}).

In Figure 4 we show the region of 250–300 meV loss where part a is the ZnO (10$\bar{1}$0) surface under a 2 × 10^{-6} torr ambient of CO and where part b is the clean ZnO surface. The pronounced feature at 280 meV loss is due to the $n = 4$ multiphonon loss of the clean surface. The apparent shift in Figure 4a relative to Figure 4b is not due to a rigid shift of the energy of the loss peak (since neither the $n = 3$ nor $n = 5$ surface phonon peaks are shifted from their clean positions due to the adsorption of CO). Rather, this is due to the superposition of a new CO induced feature (difference curve shown in Figure 4(c)) at ~273 meV (2202 cm^{-1}). (The difference curve, Figure 4c, is obtained by normalization of the intensity of Figures 4a and b to the intensity of the $n = 3$ phonon loss peak at 210 meV and subsequent subtraction.) This symmetrical loss feature at 273 ± 2 meV[13] (2202 cm^{-1}) is thus assigned to the carbon–oxygen stretching mode of the adsorbed CO. The value of 273 ± 2 meV for the fundamental is quite consistent with an anharmonicity not strongly altered by adsorption onto the surface ($\omega_e x_e$ = 13.5 cm^{-1} for a free CO molecule). It is also quite consistent with published infrared transmission data for CO adsorbed on ZnO powders where reported values for the C–O stretch are in the range of 2192–2212 cm^{-1} (depending upon surface preparation, i.e., relative degree of surface oxidation/reduction[4]). No other loss features due to CO adsorption were observed in the 200–300-meV loss region.

The final CO-derived feature in the loss spectrum is at 31 meV (250 cm^{-1}), as shown in Figure 5. This feature can only be seen for elastic peaks of optimum resolution (14–16 meV) where the tailing of the peak is at a minimum. Our previous measurements have shown that under our conditions of temperature and ambient pressure, CO adsorption is at Zn sites;[5] thus, the 31 meV feature arises from the Zn–(CO) stretch. We should note that the 31 meV (250 cm^{-1}) mode is far outside the accessible window for transmission measurements, as powdered samples are observed to become opaque below ~1000 cm^{-1}.[14]

These experimental values of the vibrational frequencies of CO on the ZnO (10$\bar{1}$0) surface are strikingly different from published results for CO on transition metal surfaces. Table I[15-19] shows some values for the metal–carbon and carbon–oxygen stretching frequencies for CO adsorbed on Pt, Cu, and Ni, as well as our results for ZnO. The two apparent differences are: (1) the increase in the stretching frequency of CO adsorbed on ZnO, as opposed to the decrease on the metals, relative to the gas-phase value; and (2) the low value of the metal–carbon stretch for CO

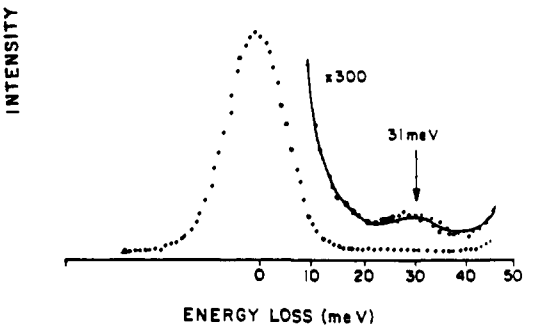

Figure 5. HREELS spectrum of the loss region of 0–50 meV; the Zn–C stretch at 31 meV is observed for the CO-covered surface at T = 100 K and CO pressure of 2 × 10^{-6} torr.

on ZnO relative to those for metals.

The adsorption of CO onto a surface atom can change the CO stretching frequency in two fundamentally different ways. First, the CO stretching mode couples mechanically to the molecule-surface atom mode of oscillation. This invariably causes an upward shift in the observed frequency.[19,20] Secondly, changes in molecular electronic structure induced by chemisorption can serve to alter the force constant of the CO bond itself. In the chemisorption of CO on metals (as well as in the analogous metal carbonyl complexes), the CO stretching frequency is invariably less than the gas-phase value, indicating that the CO bond force constant has decreased, due to π backbonding interactions with the metal.

Since our results indicate that the CO stretching frequency increases upon adsorption, it is necessary to determine whether this increase is due exclusively to the coupling between the two modes of oscillation, or whether this increase is at least in part due to a strengthened carbon–oxygen force constant. To this end we have carried out a normal mode calculation for the linear triatomic molecule M–C–O where M represents the surface. The force constants can be determined from the stretching frequencies by using the relation for the *xyz* linear triatomic molecule in Herzberg:[21] this calculation assumes a valence force field. We have assumed an infinite mass for M, corresponding to a rigid lattice. Relaxing this assumption affects the calculated metal–carbon force constant but has no significant effect on the C–O force constant.[22]

The results of this calculation for the four triatomic systems are shown in Table I. The calculated force constants for the metal systems show values below the gas-phase value of 18.56 mdyn/Å, whereas the ZnO–CO result shows an increase in the C–O force constant. This indicates that the increase in the CO stretching frequency of 50–70 cm^{-1} upon adsorption of CO to ZnO[3] is due to a strengthening of the CO bond and not solely to a mechanical coupling between the oscillations; in fact, only 13–19 cm^{-1} of the increase in CO stretching frequency[22] relates to mechanical coupling, and therefore the remaining 44 ±13 cm^{-1} relates to an

(13) The uncertainty of ±2 meV is derived from our inability to accurately subtract out the contribution of the 4th phonon loss in the region of the CO derived feature.
(14) R. J. Kokes, *Acc. Chem. Res.*, **6**, 226 (1973).
(15) H. Hopster and H. Ibach, *Surf. Sci.*, **77**, 109 (1978).
(16) B. A. Sexton, *Chem. Phys. Lett.*, **63**, 451 (1979).
(17) S. Andersson, *Solid State Commun.*, **21**, 75 (1977).
(18) R. N. Dixon, "Spectroscopy and Structure", Methuen, London, 1965.
(19) N. S. Hush and M. L. Williams, *J. Mol. Spectrosc.*, **50**, 349 (1974).
(20) T. Okawa, M. Soma, H. Bandow, and K. Uchida, *J. Catal.*, **54**, 439 (1978).
(21) G. Herzberg, "Infrared and Raman Spectra", Van Nostrand, New York, 1945, p 173.
(22) The value of the calculated CO stretching frequency using M = Zn and M = 1000 (infinite) differ by only 6 cm^{-1}.

increase in bond order of the CO molecule.

These results in combination with our earlier photoelectron studies provide a rather detailed picture of the electronic structure of the ZnO–CO surface complex shown in Figure 1. The decrease in 4σ–5σ splitting upon coordination (as observed in the He(II) photoelectron spectrum) indicates that the CO is acting as a 5σ donor, removing electron density from an orbital which is weakly antibonding with respect to the CO molecule. There is simultaneously a net donation of negative charge from the CO molecule toward the surface (as determined from He(I) photoelectron work function studies) thus indicating that little π backbonding into the $2\pi^*$ orbital of the CO molecule occurs. The net effect is to increase the CO bond order as is reflected by the increase in CO stretching frequency.

This geometric and electronic structure picture of CO on ZnO has implications concerning its reactivity, in particular with respect to the synthesis of methanol. The polarized molecule has a strengthened CO bond, initially making C–O bond rupture less probable but making the molecule susceptible to heterolytic attack by dissociated H_2, which is known to adsorb as Zn–H^- and O–H^+.[14]

Acknowledgment. Support for this work was provided by the Department of Energy under Grant De-A502-78ER04998. Also, we thank Susan Cohen for useful discussions and help with the final preparation of this manuscript.

Registry No. Carbon monoxide, 630-08-0; zinc oxide, 1314-13-2; methanol, 67-56-1.

Photophysics of Polycyclic Aromatic Molecules on Semiconductor Powders[1]

K. Chandrasekaran and J. K. Thomas*

Contribution from the Department of Chemistry, University of Notre Dame, Notre Dame, Indiana 46556. *Received March 21, 1983*

Abstract: Several aromatic molecules (pyrene, perylene, anthracene, methylanthracene, pyrenecarboxaldehyde, and bromopyrene) have been adsorbed on TiO_2 particles suspended in water. The unsubstituted arenes show significant changes in their absorption and emission spectra which comment on the nature of the adsorbed state. Substituted molecules exhibit spectra characteristic of polar environments. Coadsorption of other molecules, e.g., OH^-, I^-, or dimethylaniline, onto TiO_2 containing pyrene changes the emission spectrum to that characteristic of pyrene in a polar medium. Pulsed laser studies show that little if any movement of adsorbed molecules occurs on the TiO_2 surface. The fluorescence of adsorbed pyrene shows two well-defined time regions, one with a $t_{1/2}$ of 5 ns and the other with $t_{1/2}$ of 200 ns. The data show that at least two sites of adsorption exist for pyrene on TiO_2. The data are discussed in terms of spectroscopy established for these molecules in homogeneous solution and simple colloids such as micelles.

Introduction

The last decade has seen an increasing amount of interest in the photochemistry at interfaces,[2-5] in such systems as micelles, microemulsions, and, more recently, colloidal semiconductors.[6-12] The concept of all this work is to utilize the unique properties of the interfaces, or surfaces of these materials, in order to help to drive selected features of photochemical reactions. In particular, photoinduced electron-transfer reactions have been of prime importance because of their possible use in the storage of solar energy either as electrical energy[13] or as ionic products.[14]

Work with semiconductors has held particular appeal because of the strong photochemical properties of these materials. For example, TiO_2 colloids with very large surface areas may be prepared in aqueous solution. These colloids readily adsorb receptor molecules such as methyl viologen. On photoexcitation an electron is transferred from the semiconductor to the receptor, e.g., methyl viologen, and subsequent chemistry leads to useful products such as hydrogen, etc.[15,16]

These systems possess other features, which are slightly removed from the above type of photochemistry. For decades there has been a tremendous amount of interest in the use of catalysts to drive selected thermal reactions. Here it is recognized that the adsorption of molecules onto the active surfaces gives rise to molecules with enhanced properties, which give rise to the selected reactions that are considered to be useful.[17,18] Several different photophysical methods have been developed recently in micellar systems which enable comment to be made on the environments of molecules adsorbed on catalytic surfaces, or at active interfaces.[19-22] For example, ease of excimer formation, and quenching of excited states, comment on the movement of molecules on surfaces, the technique of fluorescence polarization comments on the local degree of rigidity of bound molecules, while fluorescence spectra of adsorbed probe molecules can comment on the environment of the polarity of molecules at sites of adsorption.[23,24] These techniques have been successfully used to study the adsorption of molecules on solid surfaces such as aluminum oxide and on silica gel.[19,25,26] This paper describes the use of selected

(1) The authors wish to thank the Petroleum Research Foundation of the American Chemical Society for support of this research.
(2) Fendler, J. H.; Fendler, E. J. "Catalysis in Micellar and Macromolecular Systems"; Academic Press: New York, 1975.
(3) Turro, N. J.; Grätzel, M.; Braun, A. *Angew. Chem.* **1980**, *19*, 675.
(4) Thomas, J. K. *Chem. Rev.* **1980**, *80*, 283.
(5) Chandrasekaran, K.; Ginnotti, C.; Monserrat, K.; Otruba, J. P.; Whitten, D. G. *J. Am. Chem. Soc.* **1982**, *104*, 6200.
(6) Grätzel, M. *Acc. Chem. Res.* **1981**, *14*, 376.
(7) Henglein, A. *Ber. Bunsenges. Phys. Chem.* **1982**, *86*, 241.
(8) Bard, A. J. *J. Photochem.* **1979**, *10*, 59.
(9) Fujishima, A.; Honda, K. *Bull. Chem. Soc. Jpn.* **1971**, *44*, 1148.
(10) Kuczynski, J.; Thomas, J. K. *Chem. Phys. Lett.* **1982**, *88*, 445.
(11) Leygrat, C.; Hendewerk, M.; Somorjai, G. A. *Proc. Natl. Acad. Sci. U.S.A.* **1982**, *79*, 5739.
(12) Sato, S.; White, M. J. *J. Phys. Chem.* **1981**, *85*, 336.
(13) Ohnishi, T.; Nakata, Y.; Tsubomura *Ber. Bunsenges. Phys. Chem.* **1979**, *79*, 523.
(14) Frank, S. N.; Bard, A. J. *J. Am. Chem. Soc.* **1977**, *99*, 303.
(15) Darwent, J. R.; Porter, G. *J. Chem. Soc., Chem. Commun.* **1981**, 145.
(16) Sato, S.; White, J. M. *Chem. Phys. Lett.* **1980**, *77*, 83.
(17) Kobayashi, J.; Yoneyama, H.; Tamura, H. *J. Electroanal. Chem.* **1982**, *138*, 105.
(18) Tinnemans, A. H. A.; Koster, T. P. M.; Thewissen, D. H. M. W.; Mackor, A. Y. *Nouv. J. Chim.* **1982**, *6*, 373.
(19) (a) Bauer, R. K.; Borenstein, R.; Mayo, P.; Okada, K.; Rafaiska, M.; Ware, W. R.; Wu, K. C. *J. Am. Chem. Soc.* **1982**, *104*, 4635. (b) Bauer, R. K.; Mayo, P.; Okada, K.; Ware, W. R.; Wu, K. C. *J. Phys. Chem.* **1983**, *87*, 460.
(20) Wheeler, J.; Thomas, J. K. *J. Phys. Chem.* **1982**, *86*, 4540.
(21) Laane, C.; Willner, I.; Otvos, J. W.; Calvin, M. *Proc. Natl. Acad. Sci. U.S.A.* **1981**, *78*, 5928.
(22) Kuczynski, J.; Thomas, J. K., submitted for publication.
(23) Kalyanasunderam, K.; Thomas, J. K. *J. Am. Chem. Soc*, **1977**, *99*, 2039.
(24) Kalyanasundaram, K.; Thomas, J. K. *J. Phys. Chem.* **1977**, *81*, 2176.
(25) Francis, C.; Lin, J.; Singer, L. A. *Chem. Phys. Lett.* **1983**, *94*, 162.

0002-7863/83/1505-6383$01.50/0